molecules

MDPI

Review

Recent Advances in Crystalline Oxidopolyborate Complexes of *d*-Block or *p*-Block Metals: Structural Aspects, Syntheses, and Physical Properties

Shu-Sheng Xin [1], Ming-Hua Zhou [1], Michael A. Beckett [2,*] and Chun-Yang Pan [1,*]

[1] School of Chemical Engineering and Light Industry, Guangdong University of Technology, Guangzhou 510006, China; xinshusheng0604@163.com (S.-S.X.); zmh1277502231@163.com (M.-H.Z.)
[2] School of Natural Sciences, Bangor University, Bangor LL57 2UW, UK
* Correspondence: m.a.beckett@bangor.ac.uk (M.A.B.); panchuny@gdut.edu.cn (C.-Y.P.)

Abstract: Crystalline materials containing hybrid inorganic–organic metal borates (complexes with oxidoborate ligands) display a variety of novel framework building blocks. The structural aspects of these hybrid metallaoxidoborates containing $Cd^{(II)}$, $Co^{(II)}$, $Cu^{(II)}$, $Ga^{(III)}$, $In^{(III)}$, $Mn^{(II)}$, $Ni^{(II)}$ or $Zn^{(II)}$ metal centers are discussed in this review. The review describes synthetic approaches to these hybrid materials, their physical properties, their spectroscopic properties and their potential applications.

Keywords: borates; coordination compounds; inorganic–organic hybrids; oxidoborate ligands

check for updates

Citation: Xin, S.-S.; Zhou, M.-H.; Beckett, M.A.; Pan, C.-Y. Recent Advances in Crystalline Oxidopolyborate Complexes of *d*-Block or *p*-Block Metals: Structural Aspects, Syntheses, and Physical Properties. *Molecules* **2021**, *26*, 3815. https://doi.org/10.3390/molecules26133815

Academic Editors: Yinghuai Zhu, Narayan S. Hosmane and Igor B. Sivaev

Received: 3 June 2021
Accepted: 18 June 2021
Published: 22 June 2021

Publisher's Note: MDPI stays neutral with regard to jurisdictional claims in published maps and institutional affiliations.

Copyright: © 2021 by the authors. Licensee MDPI, Basel, Switzerland. This article is an open access article distributed under the terms and conditions of the Creative Commons Attribution (CC BY) license (https://creativecommons.org/licenses/by/4.0/).

1. Introduction

In borate chemistry (n.b. oxidoborate is the recommended IUPAC name for oxidized oxygen containing borates [1]) the boron centers are bound to oxygen atoms as sp^2 hybridized triangular $\{BO_3\}$ (Δ) or sp^3 hybridized $\{BO_4\}$ tetrahedral (T) structural units [2–4]. These fundamental units can be aggregated, employing organic cations or transition-metal cations as templating agents [5], with condensation and oxygen atom corner sharing into larger oxidoborate clusters. In these structures, terminal oxygen atoms (i.e., those not corner shared) are generally also bound to hydrogen atoms as hydroxy groups [2–4]. Such oxidoborates are often described as hydrated borates [6] and these compounds are readily formed under relatively mild conditions [2–6]. Harsher conditions can lead to anhydrous borates and although very rare, even to the possibility of edge sharing oxygen atoms [7]. Descriptors have been developed by Christ and Clark [2] and by Burns and co-workers [4] to designate reoccurring structural motifs as framework building blocks (FBBs) and Christ and Clark's descriptors [2] are used in this review. Hydrated oxidiborates may enter the primary coordination shell of metals, with formation of *O*-donor coordinate bonds with the result of even more complex and diverse species. Coordination compounds containing oxidopolyborate ligands are therefore an important sub-class of synthetic oxidoborate compounds and recent progress in this area is the subject of this review. Since insular oxidopolyborate anions partnered by cationic transition-metal complexes do not contain oxidoborates as *ligands* they are not within the scope of this review and are excluded. Metal complexes often contain more than one ligand type and those that contain oxidoborate ligands and conventional organic ligands with typical donor atoms may also be classified as inorganic–organic hybrid materials [8,9]. Such hybrid compounds may potentially have unique and useful properties as a result of combining and/or enhancing properties associated with non-hybrid single materials.

This review is designed to be comprehensive within the defined topic and covers recently reported (twenty-first century) literature. It reports on structural chemistry, synthetic methods, physical properties and possible applications and focusses on complexes containing oxidoborate ligands. The following *d*-block and *p*-block metal ions form such

complexes: $Cd^{(II)}$, $Co^{(II)}$, $Cu^{(II)}$, $Ga^{(III)}$, $In^{(III)}$, $Mn^{(II)}$, $Ni^{(II)}$ and $Zn^{(II)}$ and subsections are dedicated to each metal. Oxidoborate ligands are discussed by increasing boron number within these metal borate subsections. Compounds containing oxidoborates ligands were first reported in the twentieth century and for information on such compounds the reader is referred to an earlier review [3] which surveys general structural aspects of oxidoborate chemistry.

2. Structural (XRD) Studies

2.1. Cadmium(II) Borates

Several oxidoborate coordination compounds of $Cd^{(II)}$ have been reported during the review period: $[Cd(dab)_{0.5}(dab')_{0.5}\{B_5O_7(OH)_3\}]_n$ (**1**) (dab = 1,4-diaminobutane) [8], $[Cd(dap)_{0.5}(dap')_{0.5}\{B_5O_8(OH)\}]_n \cdot nH_2O$ (**2**) (1,3-diaminopropane) [9], $[Cd(tren)\{B_8O_{11}(OH)_4\}]_n$ (**3**) (tren) = tris(2-aminoethyl)amine) [10], $[Cd(pn)\{B_6O_7(OH)_6\}]_n \cdot nH_2O$ (**4**) (pn = 1,2-diaminopropane) [11], $[\{Cd_3(H_2O)_4(NO_3)_2\}\{B_6O_9(OH)_2\}_2]_n$ (**5**) [12] and four related compounds, exemplified by $[pyH]_2[Cd(py)_2\{B_{14}O_{20}(OH)_6\}]$(**6**) (py = pyridine) [13].The FBB's in these compounds are mostly complex with the pentaborate(2-) unit in **1** is based on a FBB of 4(4-1) with a pendant -$B(OH)_2$ unit (FBB = 1) replacing a terminal H atom on a *T* unit of the larger FBB and can be designated a compounded descriptor 5:[4:(2Δ+2*T*)+Δ]. The FBB for **2** is based on the pentaborate(2-) unit 5:(3Δ+2*T*). The octaborate(2-) and the tetradecaborate(4-) FBBs in **3** and **6** are also best designated as compounded descriptors 8:[5:(4Δ+*T*)+3:(2Δ+*T*)] and 14:[{7:(5Δ+2*T*)}$_2$] respectively, with the latter dimer based on a FBB unit of 7. The condensed hexaborate(2-) units in **4** and **5** have a more standard descriptor based on a FBB unit of 6 i.e., 6:(2Δ+3*T*).

Compound **1** is a hybrid inorganic–organic 3-D coordination polymer [8]. The 22-electron $Cd^{(II)}$ center adopts a distorted six-coordinate octahedral complex with two *trans* *N*-donor from two different 1,4-dab ligands (forming a 1-D chain) and four *O*-donor atoms from two oxidoborate network ligands (Figure 1a).

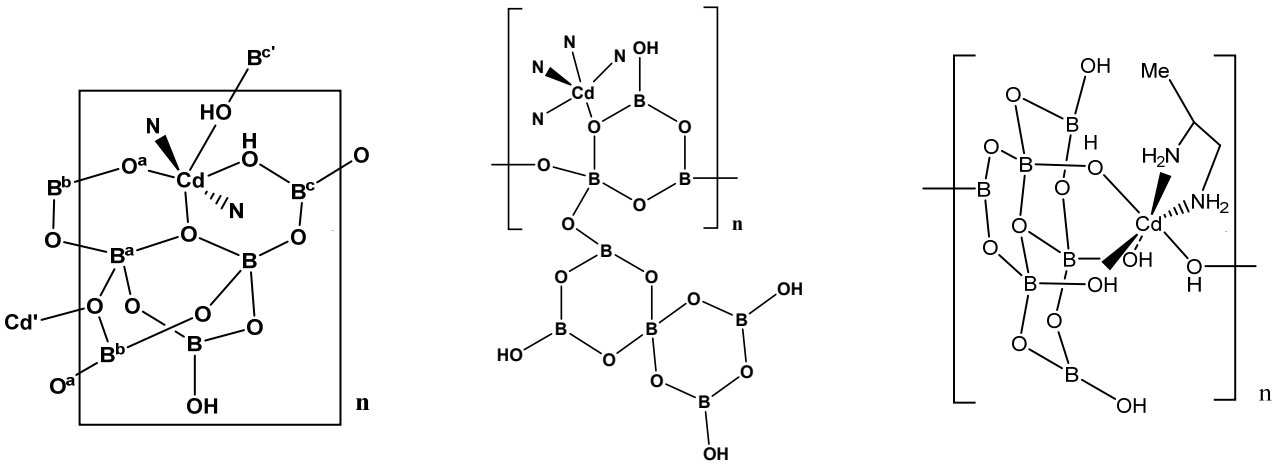

(**a**) (**b**) (**c**)

Figure 1. The building units of (**a**) $[Cd(dab)_{0.5}(dab')_{0.5}\{B_5O_7(OH)_3\}]_n$ (**1**), (**b**) $[Cd(tren)\{B_8O_{11}(OH)_4\}]_n$ (**3**), and (**c**) $[Cd(pn)\{B_6O_7(OH)_6\}]_n \cdot nH_2O$ (**4**).

Compound **2** is also a hybrid inorganic–organic 3-D coordination polymer [9]. In **2** the 2-D layers of repeating neutral $[Cd\{B_5O_8(OH)\}]$ units are linked by bridging dap units into a 3-D structure, with each 20-electron $Cd^{(II)}$ center being 5-coordinate and ligated by two monodentate *N*-donor dap ligands and three *O*-donors from the oxidoborate framework.

Compound **3** is a $Cd^{(II)}$ complex comprised of an anionic oxidoborate ligand $\{B_8O_{11}(OH)_4\}^{2-}$ fragment coordinated to a supporting $\{Cd(tren)\}^{2+}$ fragment (Figure 1b) [10]. The 20-electron $Cd^{(II)}$ center in **3** is five-coordinate and is coordinated by four *N*-donors from the tren ligand and one *O*-donor from the bridging O atom from the $\{B_3O_6(OH)\}$

sub-unit of the octaborate(2-) anion. These $\{B_3O_4(OH)\}$ sub-units, with additional pendant $\{B_5O_7(OH)_3\}$ sub-units, link together into a 1-D chain polymer. These 1-D chains are joined together into a 3-D framework via extensive H-bond interactions.

Compound **4** is an octahedral 22-electron $Cd^{(II)}$ complex with a *cis*-pn ligand and four *O*-donors from two hexaborate(2-) ligands, forming a 1-D coordination polymer chain [11]. One of the hexaborate ligands is coordinated *fac* to the $Cd^{(II)}$ center via the three OH groups bound to tetrahedral boron atoms and the final coordination bond is formed from a trigonal boron OH group from another hexaborate(2-) unit (Figure 1c). The structure of this complex is described as $[Cd(1,2\text{-dap})][B_6O_{11}(OH)_2]\cdot H_2O$ in [11] but is better formulated as $[Cd(pn)\{B_6O_7(OH)_6\}]_n\cdot nH_2O$ (**4**). The hexaborate(2-) units in **4** not only bridge two $Cd^{(II)}$ centers but are also further linked together to form an extended network which is interconnected via a strong H-bonding.

Compound **5** has a unique structure, and it is comprised of 2-D planes of condensed $\{B_6O_9(OH)_2\}^{2-}$ units coordinated to the terminal 22-electron $Cd^{(II)}$ centers of a linear $\{Cd_3(H_2O)_4(NO_3)_2\}^{4+}$ unit (Figure 2a) is such a way as to form a crosslinked 3-D network [12]. The central 22-electron $Cd^{(II)}$ center of the centrosymmetric $\{Cd_3(H_2O)_4(NO_3)_2\}^{4+}$ sub-unit (marked Cd* in Figure 2a) has two *trans* NO_3^- ligands and all three $Cd^{(II)}$ centers are octahedral with remaining sites occupied by terminal or bridging H_2O ligands or oxidoborate *O*-donor centers.

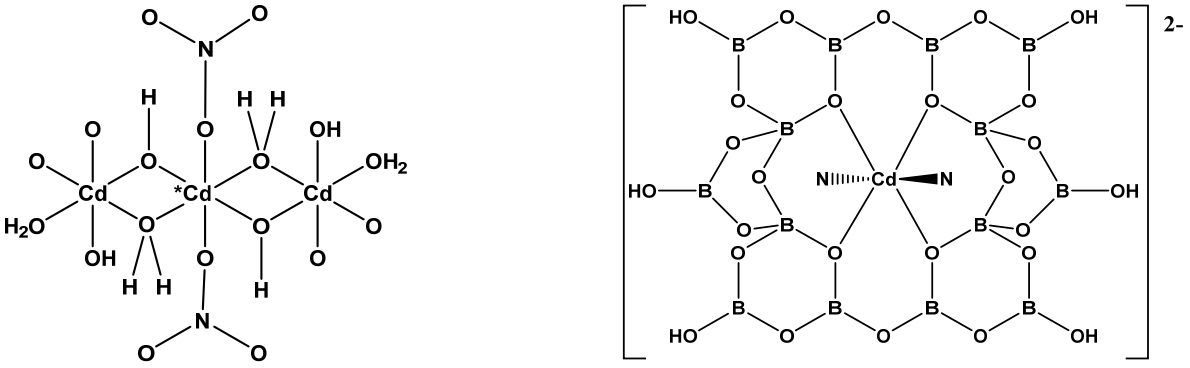

Figure 2. (**a**) The cationic $\{Cd_3(H_2O)_4(NO_3)_2\}^{4+}$ unit of $[(Cd_3)\{B_6O_9(OH)_2\}_2(NO_3)_2(H_2O)_4]_n$ (**5**). Donor atoms marked O and OH from oxidohexaborate clusters, and (**b**) the building unit of $Cd^{(II)}$-centered metallaoxidoborate cluster anion, *trans*-$[Cd(py)_2\{B_{14}O_{20}(OH)_6\}]^{2-}$ (**6**).

Compound **6** is typical of a series of four hybrid $Cd^{(II)}$ oxidoborates that exhibit 3-D open-framework with novel topologies [13]. All the networks are comprised of a novel $Cd^{(II)}$ centered complex *trans*-$[Cd(py)_2\{B_{14}O_{20}(OH)_6\}]^{2-}$ and there are further interionic links via H-bonding interactions. As shown in Figure 2b, the $[B_{14}O_{20}(OH)_6]^{4-}$ coordinates by four *O*-donors from the four boroxole $\{B_3O_3\}$ rings to the $Cd^{(II)}$ center in a square planar arrangement, with two additional axial *N*-donor ligands, resulting in a 22-electron octahedral complex.

2.2. Cobalt(II) Borates

The triborate(1-) ligand with the FBB unit of a 6-membered boroxole ring with two $\{BO_3\}$ units and one $\{BO_4\}$ unit i.e., 3:(2Δ+*T*) (Figure 3a) is present in the recently synthesized salt $[Co(H_2O)_6]_2[NO_3]_2\cdot[Co(H_2O)_4\{B_3O_3(OH)_4\}_2]\cdot 2H_2O$ (**7**) [14]. The 19-electron $Co^{(II)}$ centers are both octahedral and the two $[B_3O_3(OH)_4]^-$ ligands in the neutral $[Co(H_2O)_4\{B_3O_3(OH)_4\}_2]$ complex are *trans* and are coordinated by hydroxy *O*-donors bound to tetrahedral boron atoms.

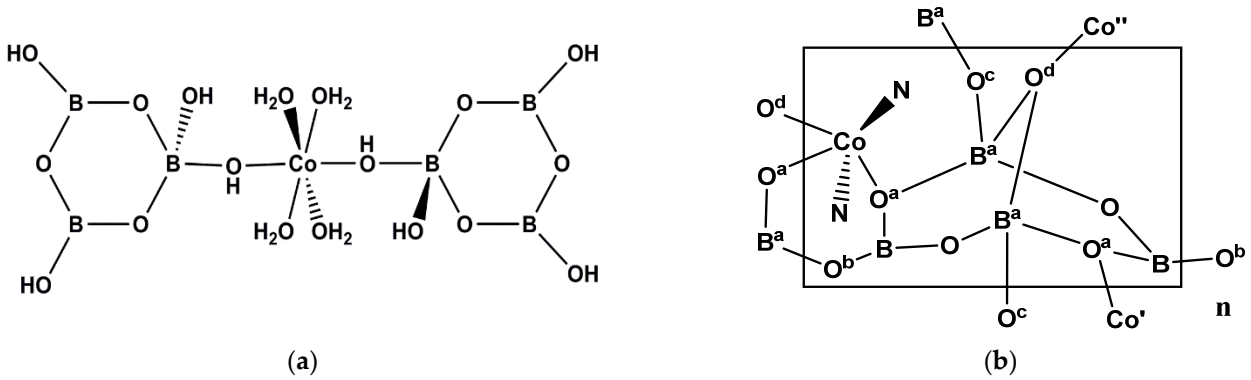

(**a**) (**b**)

Figure 3. (**a**) The structure of $[Co(H_2O)_4\{B_3O_3(OH)_4\}_2]$ (**7**), and (**b**) the building unit of $[Co(dap)_{0.5}(dap')_{0.5}\{B_4O_7\}]_n$ (**8**).

A diagram of the structure of $[Co(dap)_{0.5}(dap')_{0.5}\{B_4O_7\}]_n$ (**8**) [8] (Figure 3b) shows a five-coordinate trigonal-bipyramidal coordination geometry at the 17-electron $Co^{(II)}$ center with two *N*-donor coordinate bonds, from two different dap ligands and forming a 1-D chain, and three *O*-donor atoms from three anionic $\{B_4O_7\}^{2-}$ tetraborate units. The Christ and Clark descriptor for these units with a FBB of 4 is 4-1:(2Δ+2*T*).

The basic building unit of $[Co(tren)\{OB_5O_6(OH)_3\}]$ (**9**) is shown in Figure 4a [15]. The $[OB_5O_6(OH)_3]^{2-}$ ligand can be described as 5:(4Δ+*T*) with one of four trigonal units deprotonated. The 17-electron $Co^{(II)}$ center exhibits a trigonal-bipyramidal coordination geometry, with four *N*-donor atoms and one *O*-donor atom. Compound **9** forms 3-D supramolecular network through extensive H-bond interactions.

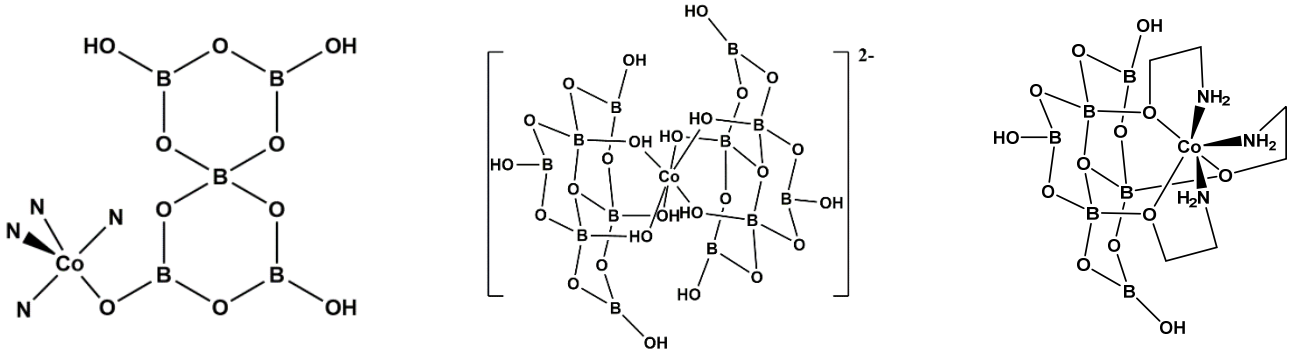

(**a**) (**b**) (**c**)

Figure 4. Drawings of (**a**) the uncharged unit of [Co(tren) $\{OB_5O_6(OH)_3\}$] (**9**), (**b**) the dianion observed in [1-cyanopiperazinium][$Co\{B_6O_7(OH)_6\}_2$]·$4H_2O$ (**11**), and (**c**) the structure of $[Co\{(NH_2CH_2CH_2O)_3B_6O_7(OH)_3\}]$ (**12**).

The homoleptic bis(hexaborate(2-))cobalt(II) complexes [piperazine-1,4-dium] $[Co\{B_6O_7(OH)_6\}_2]\cdot 6H_2O$ (**10**) [16] and [1-cyanopiperazinium][$Co\{B_6O_7(OH)_6\}_2$]·$4H_2O$ (**11**) [17] have been recently synthesized and characterized crystallographically. The oxidoborate ligands in **10** and **11** are designated 6:(3Δ+3*T*) and it is the three hydroxyl *O* atoms on the three $\{BO_4\}$ centers that coordinate in *fac*- geometries to the octahedral 19-electron $Co^{(II)}$ centers (Figure 4b). In both these structures there are strong templating interionic H-bond interactions.

The derivatized hexaborate(2-) ligand observed in $[Co\{(NH_2CH_2CH_2O)_3B_6O_7(OH)_3\}]$ (**12**) [18] has three 2-amino ethoxy groups in place of the three -OH groups on the tetrahedral boron centers of a hexaborate(2-) ion found in **10** and **11**. It functions as a hexadentate ligand through the three *O*-donors, bound to the aminoethyl substituents and the three amino *N*-donors to the 19-electron $Co^{(II)}$ center (Figure 4c).

2.3. Copper(II) Borates

Oxidoborates coordinated to $Cu^{(II)}$ centers are not uncommon and are available for diborate(2-), pentaborate(1-), hexaborate(2-) and icosaborate(12-) anions. The diborate(2-) anion is observed as part of the templated oxidoborate found in $[H_3O]_4[Cu_7(NH_3)_2(H_2O)_4\{B_{24}O_{39}(OH)_{12}\}]\cdot 13H_2O$ (**13**) [19] and this will be discussed later in this sub-section.

As shown in Figure 5a, $[Cu(pn)_2\{B_5O_6(OH)_4\}][B_5O_6(OH)_4]\cdot 4H_2O$ (**14**) [20] is an ionic compound comprised of a cationic hybrid $Cu^{(II)}$ complex containing a pentaborate(1-) ligand based on a FBB of 5:(4Δ+*T*). This +1 cation is partnered with an additional insular $[B_5O_6(OH)_4]^-$ anion. The 19-electron $Cu^{(II)}$ ion in **14** has a distorted square-based pyramidal geometry with four *N*-donor atoms, and an axial *O*-donor pentaborate(1-) with a T^5 [21] of 0.87. A sixth O-donor H_2O potential 'ligand' is axially *trans* to the pentaborate(1-) ligand, but the Cu-O distance is not within normal (or even long) bonding distances.

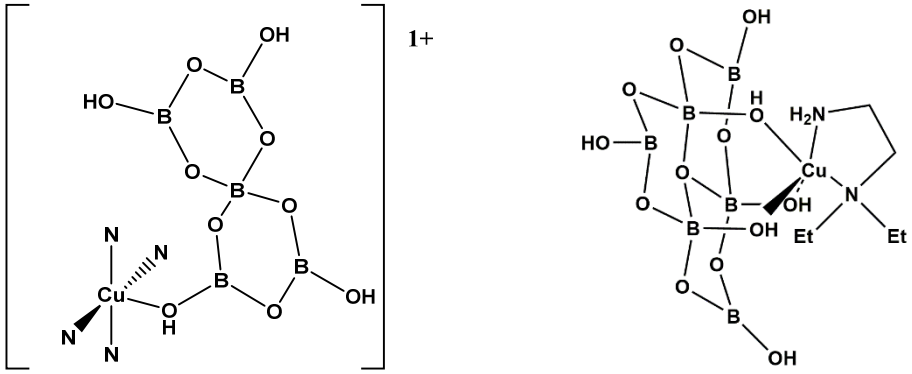

Figure 5. (**a**) The cation present in $[Cu(pn)_2\{B_5O_6(OH)_4\}][B_5O_6(OH)_4]\cdot 4H_2O$ (**14**), and (**b**) the uncharged building unit of $[Cu(deen)\{B_6O_7(OH)_6\}]\cdot 5H_2O$ (**19**).

Coordinated hexaborate ligands are well represented in $Cu^{(II)}$ coordination chemistry as illustrated by the following examples: $[Cu(NH_3)_2\{B_6O_7(OH)_6\}]_n\cdot 2nH_2O$ (**15**) [22], $[Cu(en)\{B_6O_7(OH)_6\}]_n\cdot 3nH_2O$ (**16**) (en = 1,2-diaminoethane) [23], $[Cu(dmen)\{B_6O_7(OH)_6\}]\cdot 4H_2O$ (**17**) (dmen = *N*,*N*-dimethyl-1,2-diaminoethane) [20], $[Cu(tmeda)\{B_6O_7(OH)_6\}]\cdot 6H_2O$ (tmeda = *N*,*N*,*N*′,*N*′-tetramethyl-1,2-diaminoethane) (**18**) [20], and $[Cu(deen)\{B_6O_7(OH)_6\}]\cdot 5H_2O$ (**19**) (deen = *N*,*N*-diethyl-1,2,-diaminoethane) [22]. The organic *N*-donor ligands in **17**, **18** and **19** are relatively sterically demanding and the resulting neutral coordination complexes have square-based pyramidal 5-coordinate 19-electron $Cu^{(II)}$ geometries. Each $Cu^{(II)}$ center is coordinated by two *N*-donors and three *O*-donors from the oxidohexaborate(2-) ligands. This is illustrated in Figure 5b for **19**. The organic *N*-donor ligands in **15** and **16** are relatively small and this permits the $Cu^{(II)}$ centers to adopt 6-coordinate tetragonally distorted octahedral geometries with the formation of additional Cu-O coordinate bonds from bridging oxidoborate ligands, in a similar way to that observed in the $Cd^{(II)}$ complex, **4**. These 21-electron $Cu^{(II)}$ centers are coordinated by two *N*-donors ligands, three *O*-donors from the *fac*-hexaborate(2-) ligand with a sixth site from an *O*-donor of an 'adjacent' hexaborate(2-) by formation of a 1-D coordination polymeric chain.

Three new examples of $Cu^{(II)}$ complexes containing oxidoicosaborate(12-) ligands have been prepared: $[H_3O]_4[Cu_7(NH_3)_2(H_2O)_4\{B_{24}O_{39}(OH)_{12}\}]\cdot 13H_2O$ (**13**) [19], $H_6[Cu_4O\{B_{20}O_{32}(OH)_8\}]\cdot 25H_2O$ (**20**) [24] and $H_6[Cu_4O\{B_{20}O_{32}(OH)_8\}]\cdot 34H_2O\cdot 8B(OH)_3$ (**21**) [24]. These three compounds are fundamentally structurally identical to $Cu^{(II)}$/oxidoicosaborate(6-) complexes $HM_5[Cu_4O\{B_{20}O_{32}(OH)_8\}]\cdot 32H_2O$ (M = Na, K) first synthesized by Heller and described in his early (1986) borate structural chemistry review [3]. The structure of the anion in **13**, **20** and **21** is drawn in Figure 6. It is best described as comprised on four square planar 17-electron $Cu^{(II)}$ ions and a central μ_4-O^{2-} ion supporting and surrounded by large oxidoicosaborate(12-) ring structure. This ring structure itself is 'tetrameric' with four alternating FBB's of {B1} and {B4} sub-units linked into a larger 24-membered ring with

a compound designation of 20:{4:(2Δ+2*T*)+Δ}$_4$. Compound **21** has 8 additional B(OH)$_3$ molecules per oxidoicosaborate(12-) moiety, and these are situated within channels which are available within the giant structure formed by close-packing the large multi-metallic oxidoborate anions [24].

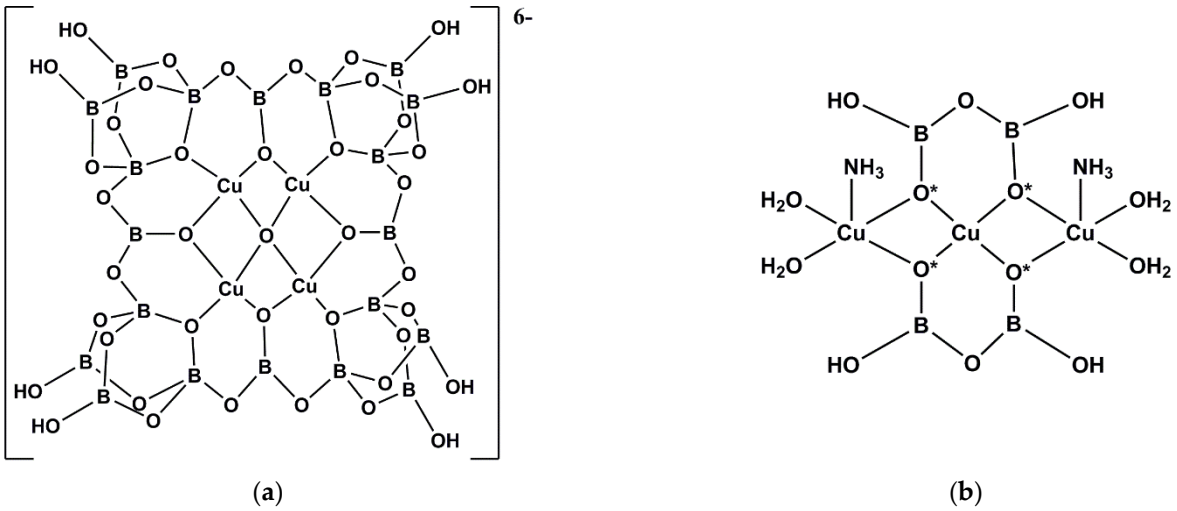

Figure 6. Drawing of (**a**) the structure of the (oxidotetracopper)oxidoicosaborate(6-) anion, $[Cu_4O\{B_{20}O_{32}(OH)_8\}]^{6-}$, found in **13**, **20** and **21**, and (**b**) the 'top layer' of **13** which is comprised of a linear $\{Cu_3\}^{6+}$ chain and two coordinated oxidodiborate(2-), $[B_2O_3(OH)_2]^{2-}$, anions. The four O* atoms also bridge to the four Cu atoms in the lower level of **13**.

Compound **13** is unique and contains seven Cu$^{(II)}$ centers. It can be considered to be a large anion based on two 'layers': the 'lower layer' is as is illustrated in Figure 6a and this layer supports a linear $\{Cu_3\}^{6+}$ unit in an 'upper layer'. The $\{Cu_3\}^{6+}$ unit is further supported by two peripheral diborate(2-) anions, and all seven 19-electron Cu$^{(II)}$ centers are 5-coordinate square-based pyramids. This 'top layer' of **13** is illustrated in Figure 6b. Structurally, compound **13** has another unusual feature: the presence of B-O$^-$ groups. It is very rare for oxidiborates prepared and crystallized from aqueous solution to display B-O$^-$ groups arising from trigonal B centers [2]. It is also interesting to note that all such B-O$^-$ groups in the 'upper layer' of **13** are found bridging two (μ_2-) or three (μ_3-) Cu$^{(II)}$ centers and that the central O^{2-} ion bridges five (μ_5-) Cu$^{(II)}$ centers [19]. There are also four B-O$^-$ groups in the 'lower layer' of **13**, and in **20** and **21** that each bridge (μ_2-) two Cu$^{(II)}$ centers.

2.4. Gallium(III) and Indium(III) Borates

Ga$^{(III)}$ and In$^{(III)}$ borates are conveniently considered together. The hybrid oxidoborate, $[Ga(en)_2\{B_5O_8(OH)_2\}]_n \cdot nH_2O$ (**22**) was first synthesized in 2012 [25]. The two en *N*-donor bidentate ligands occupy four coordination sites around an octahedral 22-electron Ga$^{(III)}$ center and the two remaining *cis*- coordination sites are connected to two different $\{B_5O_8(OH)_2\}^{3-}$ anions forming a 1-D chain structure (Figure 7a). Two recently reported compounds $[Ga(teta)\{B_5O_8(OH)_2\}]_n \cdot nH_2O$ (**23**) (teta = tetraethylenetriamine) and $[In(teta)\{B_5O_8(OH)_2\}]n \cdot 1.5nH_2O$ (**24**) have similar structures [11]. Compound **22** was also reported in 2013 together with three other related compounds: $[In(en)_2\{B_5O_8(OH)_2\}] \cdot H_2O$ (**25**), $[In(dap)_2\{B_5O_8(OH)_2\}] \cdot H_2O$ (**26**), and $[In(dien)\{B_5O_8(OH)_2\}]_n$ (**27**) [26]. The structures of **25** and **26** are essentially the same as **22** with a change of metal (to In$^{(III)}$ in **25**) or ligand and metal (to In^{III} and dap in **26**). Compounds **22**–**27** contain $\{B_5O_8(OH)_2\}^{3-}$ anions and these anions are based on the frequently observed 5:(4Δ+*T*) pentaborate(1-) anion, $[B_5O_6(OH)_4]^-$, but is additionally double deprotonated. The related compound $Rb_{2n}[Ga\{B_5O_{10}\}]_n \cdot 4nH_2O$ (**28**) has also been reported [25]. Here, the 5:(4Δ+*T*) building block is deprotonated 4 times to form the $[B_5O_{10}]^{5-}$ anion with four of these anions coordinated to a tetrahedral 18-electron Ga$^{(III)}$ center in chain-like 2-D structures.

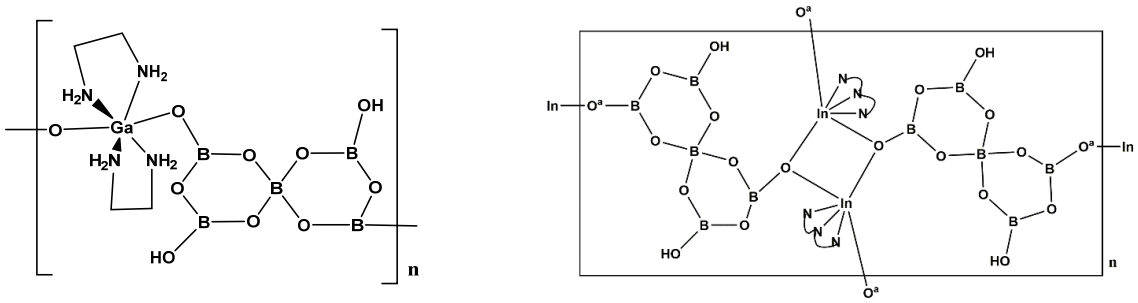

Figure 7. The building unit of (**a**) $[Ga(en)_2\{B_5O_8(OH)_2\}]_n \cdot nH_2O$ (**22**), and (**b**) the dimeric $In^{(III)}$ centers in $[In(dien)\{B_5O_8(OH)_2\}]_n$ (**27**).

Compound **27** is unique and features octahedral $In^{(III)}$ centers coordinated by a tridentate dien ligand (*fac*-) and three monodentate $\{B_5O_8(OH)_2\}^{3-}$ ligands which bridge to other $In^{(III)}$ centers in such a way as to produce a 'dimeric' 1-D chain with oxidoborate *O*-bridges between two $In^{(III)}$ centers (Figure 7b). The H-bonding interactions between adjacent chains leads to a supramolecular H-bonded network.

2.5. Manganese(II) Borates

One 15-electron five-coordinate trigonal-bipyramidal $Mn^{(II)}$ complex with a coordinated oxidoborate ligand has been reported, $K_7[(BO_3)Mn\{B_{12}O_{18}(OH)_6)\}]\cdot H_2O$ (**29**) [27]. The structure of this will be discussed in Section 2.7 since **29** is isostructural with an analogous 20-electron $Zn^{(II)}$ complex and forms part of a family of structurally related of $Zn^{(II)}$ compounds.

2.6. Nickel(II) Borates

The recently synthesized salt $[Ni(H_2O)_6]_2[NO_3]_2\cdot[Ni(H_2O)_4\{B_3O_3(OH)_4\}_2]\cdot 2H_2O$ (**30**) [14] is isostructural with **7**. The two $[B_3O_3(OH)_4]^-$ ligands in the neutral $[Ni(H_2O)_4\{B_3O_3(OH)_4\}_2]$ complex are *trans* on octahedral 20-electron $Ni^{(II)}$ centers and are coordinated by hydroxy *O*-donors bound to tetrahedral boron atoms of the triborate(1-) anion.

Two $Ni^{(II)}$ hexaborate(6-) complexes have recently been synthesized during the review period: $[Ni(en)(H_2O)_2\{B_6O_7(OH)_6\}]\cdot H_2O$ (**31**) [28] and $[Ni(dmen)(H_2O)\{B_6O_7(OH)_6\}]\cdot 5H_2O$ (**32**) [28]. These compounds are neutral molecules and contain the $[B_6O_7(OH)_6]^{2-}$ ligand as described earlier for **4**, **10, 11** and **15–19** (Sections 2.1–2.3). These ligands are also found in $Zn^{(II)}$ chemistry (Section 2.7). Both **31** and **32** are octahedral about the 20-electron $Ni^{(II)}$ centers but differ in the denticity of the hexaborate(2-) ligands which are bidentate in **31** (Figure 8a) and tridentate in **32**. Both compounds demonstrate numerous intermolecular and intramolecular solid-state structure directing H-bond interactions.

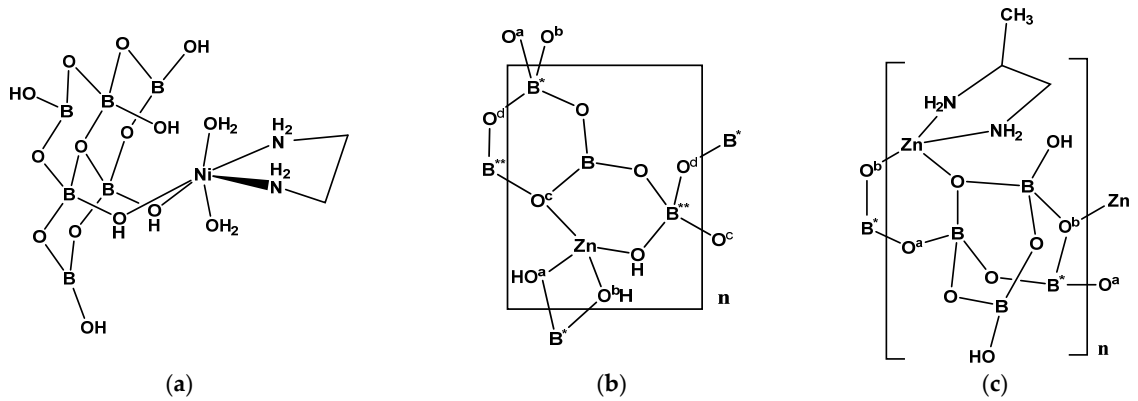

Figure 8. (**a**) The uncharged complex of $[Ni(en)(H_2O)_2\{B_6O_7(OH)_6\}]\cdot H_2O$ (**31**) showing the bidentate nature of the $[B_6O_7(OH)_6]^{2-}$ ligand, (**b**) the building unit of $[Zn\{B_3O_4(OH)_3\}]_n$ (**35**), and (**c**) the building unit of $[Zn(pn)\{B_4O_6(OH)_2\}]_n$ (**36**).

The derivatized hexaborate(2-) ligand, with three 2-amino ethoxy groups, in place of the three -OH groups on the tetrahedral boron centers, functions as a hexadentate ligand in the 20-electron $Ni^{(II)}$ complex, $[Ni(NH_2CH_2CH_2O)_3\{B_6O_7(OH)_3\}]$ (**33**) [18]. Compound **33** is isostructural with **12**.

2.7. Zinc(II) Borates

There have been more oxidoborate complexes reported for $Zn^{(II)}$ than for any other metal. The coordinated oxidoborate ligands range in size from triborate(1-) to dodecaborate(6-).

The recently synthesized salt $[Zn(H_2O)_6]_2[NO_3]_2\cdot[Zn(H_2O)_4\{B_3O_3(OH)_4\}_2]\cdot 2H_2O$ (**34**) [14] is isostructural with **7** and **30**. The two $[B_3O_3(OH)_4]^-$ ligands in the neutral $[Zn(H_2O)_4\{B_3O_3(OH)_4\}_2]$ complex are *trans* on octahedral 22-electron $Zn^{(II)}$ centers and are coordinated by hydroxy *O*-donors bound to tetrahedral boron atoms.

Structural characterization of the commercially important $Zn^{(II)}$ triborate, $[Zn\{B_3O_4(OH)_3\}]_n$ (**35**), revealed that it was a crosslinked 1-D coordination chain polymer of $Zn^{(II)}$ [29]. The oxidoborate forms a 1-D polymeric chain (Figure 8b) and each 18-electron $Zn^{(II)}$ center is coordinated by two oxygen atoms from two adjacent monomeric unit of the chain, and completes its tetrahedral arrangement by coordination from two hydroxide *O*-donors from a neighboring chain to crosslink the structure into a 2-D network. The network also has numerous interchain H-bond interactions. Each triborate(2-) FBB unit is a 6-membered boroxole ring with one $\{BO_3\}$ and two $\{BO_4\}$ units, i.e., 3:(Δ+2*T*).

Tetraborate ligands based on the 4(4-1) FBB are represented by the following compounds $[Zn(pn)\{B_4O_6(OH)_2\}]_n$ (**36**) [30], $[Zn(dap)_{0.5}(dap')_{0.5}\{B_4O_6(OH)_2\}]_n\cdot nH_2O$ (**37**) [30], and $[Zn(dab)_{0.5}(dab')_{0.5}\{B_4O_6(OH)_2\}]_n\cdot nH_2O$ (**38**) [31]. Compounds **36-38** have identical $Zn^{(II)}$/ligand/borate stoichiometries with similar, but non-identical, structures. All three contain tetrahedral 18-electron $Zn^{(II)}$ centers with two *N*-donor amine and two *O*-donor tetraborate ligands, with the latter condensed into 1-D tetraborate chains. Compound **36** contains a chelating pn ligand (Figure 8c) whereas **37** (and **38)** has two dap (or dab) ligands on each $Zn^{(II)}$ center both bridging other $Zn^{(II)}$ centers and forming a 1-D coordination polymer chains in crosslinked inorganic–organic 2-D layered structures.

The FBB of 5:(4Δ+*T*) is present in $[Zn(tren)\{B_5O_7(OH)_3\}]$ (**39**) [32] and this ligand is identical to that found in **9** (Section 2.2). $[Zn(dab)_{0.5}(dab')_{0.5}\{B_5O_7(OH)_3\}]_n$ (**40**) [8] and $[Zn(appip)\{B_4O_6(OH)(OB\{OH\}_2\})]_n\cdot 3nH_2O$ (**41**) (appip = *trans*-1,4-bis(3-aminopropyl) piperazine) [30] are based on a FBB of 4 with a pendant $-OB(OH)_2$ replacing a hydroxyl group on a tetrahedral boron center of the tetraborate moiety with a 5:[4:(2Δ+2*T*)+Δ] framework and are isostructural with **1** (Section 2.1).

The 6:(3Δ+3*T*) FBB, described in Sections 2.1–2.3 and 2.6, is also observed as a hexaborate(2-) ligand in $Zn^{(II)}$ complexes. The following complexes have been prepared $[Zn(dien)\{B_6O_7(OH)_6\}]\cdot 0.5H_2O$ (**42**) [33], $(NH_4)_2[Zn(H_2O)_2\{B_6O_7(OH)_6\}_2]\cdot 2H_2O$ (**43**) [33], $[Zn(en)\{B_6O_7(OH)_6\}]_n\cdot 2nH_2O$ (**44**) [34] and $[Zn(pn)\{B_6O_7(OH)_6\}]_n\cdot 1.5nH_2O$ (**45**) [34]. The 22-electron $Zn^{(II)}$ centers in **42**-**45** are all octahedral with N_3O_3, O_6, N_2O_4 and N_2O_4 donor sets, respectively. The hexaborate(2-) ligands in **42**, **44** and **45** are tridendate but are bis(bidentate) and *trans* in the centrosymmetric anion in **43** (Figure 9a). Compounds **44** and **45** are 1-D coordination polymers with a -OH group of a trigonal boron of the coordinated hexaborate(2-) anion bridging onto another $Zn^{(II)}$ center. This configuration has also been observed in $Cd^{(II)}$ (**4**, Section 2.1) and $Cu^{(II)}$ (**15** and **16**, Section 2.3) chemistry.

$\{\{Zn(en)_2B_7O_{10}(OH)_3\}_2\}_n$ (**46**), also formulated as $[Zn(en)_2\{B_7O_{12}(OH)\}]$ in Ref. [9], is a 3-D coordination polymer comprised of an octahedrally coordinated 22-electron $Zn^{(II)}$ center based on square planar $[Zn(en)_2]$ units axially coordinated by a *O*-donor condensed oxidoheptaborate framework. The oxidoborate FBB in **46**, $[B_7O_{10}(OH)_3]_n^{2n-}$, can be described by a compounded descriptor 7:[(3:2Δ+*T*)+(3:2Δ+*T*)+Δ] with triangular $BO_2(OH)$ cross-linking units (Figure 9b).

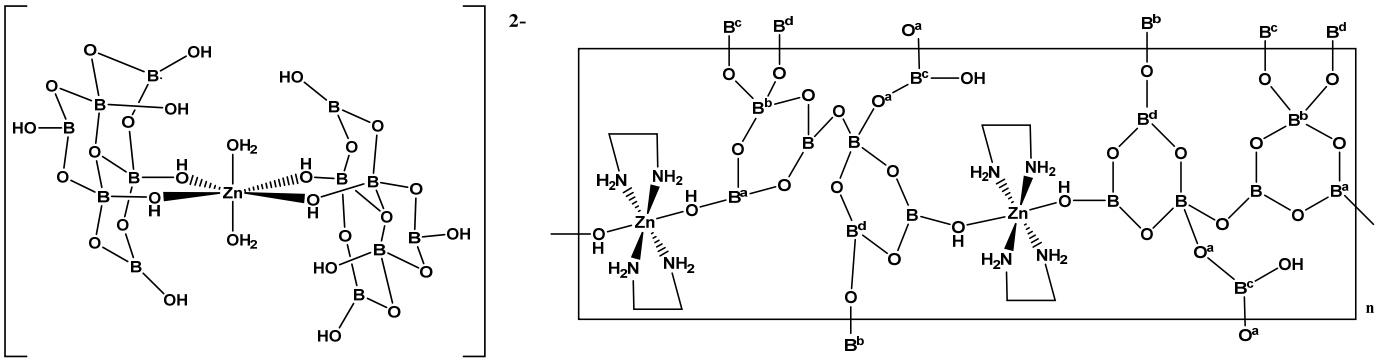

(**a**) (**b**)

Figure 9. Drawings of (**a**) the insular anion in $(NH_4)_2[Zn(H_2O)_2\{B_6O_7(OH)_6\}_2]\cdot 2H_2O$ (**43**), and (**b**) the repeating unit of $[\{Zn(en)_2\{B_7O_{10}(OH)_3\}_2]_n$ (**46**).

$[Zn(en)_2\{B_8O_{11}(OH)_4\}]_n$ (**47**) [10] was reported in 2017 and has a similar stoichiometry to **3** but is isomeric, with a different oxidoborate condensation mode and a 1-D polymer chain. (Figure 10a). Nevertheless, the octaborate(2-) anion is best designated by the compounded descriptor 8:[5:(4Δ+*T*)+3:(2Δ+*T*)].

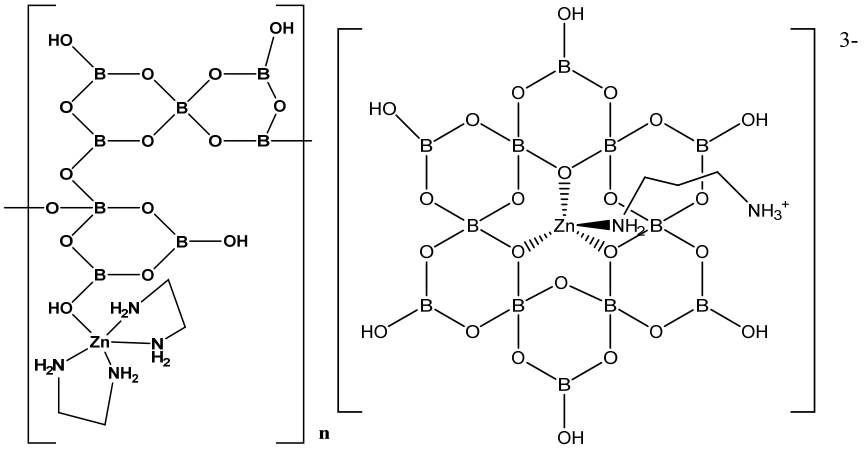

(**a**) (**b**)

Figure 10. (**a**) The repeating unit of $[Zn(en)_2\{B_8O_{11}(OH)_4\}]_n$ (**47**), and (**b**) a drawing of the $[(Hdap)Zn\{B_{12}O_{18}(OH)_6\}]^{3-}$ anion in $(H_2dap)_3[(Hdap)Zn\{B_{12}O_{18}(OH)_6\}]_2\cdot 14H_2O$ (**51**).

$[Zn_2(dap)(dap')\{B_8O_{13}(OH)_2\}]_n$ (**48**) [30] has a similar structure to **37** and **38** with the 18-electron $Zn^{(II)}$ centers tetrahedral with 2 monodentate bridging dap *N*-donor ligands. The octaborate(4-) *O*-donor ligands are based on two condensed tetraborate(2-) building blocks via an O bridge, 8:{4(2Δ+2*T*)}$_2$. However, this now results in 2-D layers rather than 1-D chains and the 2-D layers are further crosslinked into 3-D networks, by the amines.

The large insular anion $[B_{12}O_{18}(OH)_6]^{6-}$ has been reported in $K_7[(BO_3)Zn\{B_{12}O_{18}(OH)_6\}]\cdot H_2O$ (**49**) [35], $[(Hen)Zn\{B_{12}O_{18}(OH)_6\}Zn(en)(Hen)]\cdot 8H_2O$ (**50**) [36] and $(H_2dap)_3[(Hdap)Zn\{B_{12}O_{18}(OH)_6\}]_2\cdot 14H_2O$ (**51**) [33]. The dodecaborate(6-) anion is based on a hexameric FBB of 3 i.e., 12:{3:(Δ+2*T*)}$_6$, with all tetrahedral boron centers linking boroxole $\{B_3O_3\}$ rings, generating a larger inner 12-membered B/O alternating B_6O_6 ring. Stereochemically, three of these potential *O*-donor atoms point to one side of the large ring and three face towards the other side. The anion in **51**, $[(Hdap)Zn\{B_{12}O_{18}(OH)_6\}]^{3-}$, which is typical of the oxidoborate building blocks contained within these structures, has a tetrahedral 18-electron $Zn^{(II)}$ center coordinated by *fac O*-donors from the dodecaborate(6-) ligand and a monodentate *N*-donor from a protonated 1,3-diamminopropane ligand (Figure 10b). There is extensive H-bonding between anions forming a supramolecular 3-D H-bonded lattice.

3. Synthetic Methods

3.1. Slow Crystallization by Solvent Evaporation

This method involves slow crystallization from aqueous or a miscible aqueous/organic solution which originally contained $B(OH)_3$ and metal precursor complexes. The oxidoborate compounds are templated by the transition-metal/p-block metal complexes present in the dynamic combinatorial library (DCL) of oxidoborate anions that are present in solution in equilibrium concentrations [37]. Products are generally under thermodynamic control especially when metal-ligand exchange equilibria (and hydroxyoxidoborate-H_2O equilibria) are fast. The solvents used for evaporation in the boric acid solution are often H_2O or H_2O/EtOH or H_2O/MeOH. Crystallization of the product may take a few hours to several weeks. This is illustrated for the preparation of $[Cu(en)\{B_6O_7(OH)_6\}]_n \cdot 3nH_2O$ (**16**) from $[Cu(en)_2]SO_4$ and $B(OH)_3$ [20]. $[Cu(en)_2]SO_4$ (3.6 mmol) and $BaSO_4 \cdot 8H_2O$ (3.6 mmol) were dissolved in H_2O (20 mL). The solution was stirred for 20 min at room temperature and the precipitate that formed ($BaSO_4$) was removed by filtration. $B(OH)_3$ (25 mmol) was added to the filtrate which was then stirred for 40 min. The resulting solution was left in several small vials to crystallize. After standing for 35 days the product **16** was collected by filtration as blue crystals in 31% yield. Compounds **11**, **13–19**, **31**, **32**, **35, 42–45**, **50** and **51** were prepared by a method similar to this. Oxidopolyborates prepared by this method are often insular salts and are often less condensed than those prepared by the methods described below, which generally use more forcing conditions.

3.2. Solvothermal/Hydrothermal Methods

Many organic-inorganic oxidoborates described in this article are synthesized by solvothermal (or hydrothermal) methods. In this method the non-aqueous solvent (or H_2O) is placed in a sealed reaction vessel together with boron containing materials, transition-metal/p-block metal salts and organic ligands and heated to a specific temperature (usually 100–250 °C) for a set time period. Solvothermal reactions can lead to metastable, kinetically controlled, products. This method is illustrated by the preparation of $[Cd(dap)_{0.5}(dap')_{0.5}\{B_5O_8(OH)\}]_n \cdot nH_2O$ (**2**) [9]. H_3BO_3 (5 mmol) and $Cd(NO_3)_2 \cdot 4H_2O$ (1 mmol) were slowly added to a *N*,*N*-dimethylformamide (2 mL) and 1,3-dap (1 mL) solution with stirring. The white emulsion was then sealed in a Teflon-lined 25 mL autoclave reactor and heated at 180 °C for 7 days. After cooling to room temperature, crystals of **2** (36% yield based on H_3BO_3) were collected by filtration, washed with H_2O, and dried in air. Compounds **1–6, 8, 9, 12, 20–29, 33, 36–41** and **46–49** were prepared by this general method. This relatively low temperature hydrothermal method is popular among many researchers since the necessary autoclave reactors are widely available in both academic and industrial laboratories.

3.3. Molten Salt Methods

In this method a molten salt (120–250 °C) is used as both solvent and reactant and the reaction vessel is charged with $B(OH)_3$ and any other necessary reaction materials. This is illustrated by the preparation of $[Co(H_2O)_6]_2[NO_3]_2 \cdot [Co(H_2O)_4\{B_3O_3(OH)_4\}_2] \cdot 2H_2O$ (**7**) [14]. $Co(NO_3)_2 \cdot 6H_2O$ (1 mmol) was placed in a 25 mL beaker and heated in an oil bath at 120 °C until fully molten (*ca.* 1 min). H_3BO_3 (0.8 mmol) was then added, and the mixture was stirred until the H_3BO_3 was completely dissolved (*ca*. 30 min). The solution was then allowed to cool to room temperature and left to crystallize. After 14 days, transparent colorless crystals of **7** (30% based on H_3BO_3) were deposited on the bottom of the beaker. Compound **7** was isolated by filtration. Compounds **30** and **34** were also prepared by this method.

4. Physical, Spectroscopic Properties and Potential Applications

The oxidoborate complexes described in this manuscript are all crystalline solids with high melting (or decomposition) points. Techniques used to characterize the oxidoborates and to study their possible applications include structural studies (single-crystal XRD,

powder-XRD, TEM), optical properties (diffuse reflectance spectroscopy, nonlinear optical studies (NLO), photoluminescence), magnetic properties, vibrational spectroscopy, thermal studies and catalytic investigations.

Oxidoborate complexes derived from transition-metals are generally colored but the d^{10} ions ($Cd^{(II)}$, $Zn^{(II)}$, $Ga^{(III)}$ and $In^{(III)}$) are colorless. UV/Vis absorption properties of several oxidopolyborate complexes (**1**, **4**, **5**–**8**, **22**–**24**, **28**, **30**, **34**, **36**, **37**, **40**, **41**) have been studied by diffuse reflectance spectroscopy and band-gaps with energies of ranging from 3.1 eV for $[(Cd_3)\{B_6O_9(OH)_2\}_2(NO_3)_2(H_2O)_4]_n$ (**5**) to 5.9 eV for $[Cd(dab)_{0.5}(dab')_{0.5}\{B_5O_7(OH)_3\}]_n$ (**1**) have been noted.

The band-gaps of $[Cd(pn)\{B_6O_7(OH)_6\}]_n{\cdot}nH_2O$ (**4**), $[Ga(teta)\{B_5O_8(OH)_2\}]_n{\cdot}nH_2O$ (**23)** and $[In(teta)\{B_5O_8(OH)_2\}]n{\cdot}1.5nH_2O$ (**24**) show interesting but different temperature effects. Compounds **23** and **24** exhibited blue maximum luminescence at 446 and 472 nm, respectively, when excited at 352 and 342 nm, respectively. The luminescence intensity of these two compounds increased with a decreasing temperature and was at its most intense at 80 K. Compound **4** exhibited the maximum luminescence at 444 nm with a 360 nm excitation light source, and the luminescence intensity increased with the decrease of temperature to 230 K where it was at its most intense. The luminescence intensity of **4** decreased when the temperature was further lowered to 80 K [11]. Compounds $[M(dab)_{0.5}(dab')_{0.5}\{B_5O_7(OH)_3\}]_n$ (M = Cd, **(1)**; M = Zn (**40**)) have been shown to display blue luminescence with maximum fluorescent emission at 423 and 412 nm, when excited at and 356 or 384 nm, with lifetimes of 4.67 and 4.09 ns, for **1** and **40**, respectively [8]. It is reported that the blue luminescence of two compounds originates from their inorganic oxidoborate frameworks.

Nonlinear optical (NLO) effects are also displayed by the following hybrid metal oxidoborates $Rb_{2n}[Ga\{B_5O_{10}\}]_n{\cdot}4nH_2O$ (**28**) [25], $K_7[(BO_3)Mn\{B_{12}O_{18}(OH)_6)\}]{\cdot}H_2O$ (**29**) [27], $[Zn(pn)\{B_4O_6(OH)_2\}]_n$ (**36**) [30] and $[Zn(appip)\{B_4O_6(OH)(OB\{OH\}_2\})]_n{\cdot}3nH_2O$ (**41**) [30]. For example, compound **41** belongs to the space group $P2_1$, and since this point group is non-centrosymmetric **41** might be expected to exhibit second order nonlinear optical effects; indeed, powdered **41** does exhibit SHG behavior with a response of 29 mV using a laser of beam energy with 2.83 mJ/pulse [30]. Compound **36** had a response of 24 mV while the response of the SHG standard, KH_2PO_4 (KDP), was 175 mV under similar conditions [30]. Compound **28** crystallizes in chiral space group $C222_1$. SHG measurements on a Q-switched Nd:YAG laser with sieved powdered samples (70−100 mesh) revealed that compound **28** displays a moderately strong SHG response approximately equal to that KDP [25]. The SHG response of **29** was again moderate and equal to that of KDP [27].

Many of the compounds described within this review are diamagnetic but those containing $Cu^{(II)}$ (**13**–**21**) and $Ni^{(II)}$ (**31**–**32**) centers are paramagnetic. The magnetic properties of the $Ni^{(II)}$ complex **30** have not been reported. Magnetic properties of the $Co^{(II)}$ (**7**–**12**) and the $Mn^{(II)}$ (**29**) oxidoborate complexes were also not reported, although these would be expected to be paramagnetic. The μ_{eff} values (per $Cu^{(II)}$ atom) of the multi-metallic complexes $[H_3O]_4[Cu_7(NH_3)_2(H_2O)_4\{B_{24}O_{39}(OH)_{12}\}]{\cdot}13H_2O$ (**13**), $H_6[Cu_4O\{B_{20}O_{32}(OH)_8\}]{\cdot}25H_2O$ (**20**) and $H_6[Cu_4O\{B_{20}O_{32}(OH)_8\}]{\cdot}34H_2O{\cdot}8B(OH)_3$ (**21**) are much lower than expected by the spin-only formula and **20** and **21** are temperature dependent and display antiferromagnetic behavior [24].

A complex borate, $[Ni(en)_3]_n[Hen]_n[B_9O_{13}(OH)_4]_n{\cdot}nH_2O$, containing isolated cations and a partially condensed anionic a one-dimensional oxidoborate chain has ferroelectric properties at room temperature [38]. The electrical hysteresis loop was observed when an electric field between −28 and +28 kV was applied to the sample. Spontaneous polarization (P_s of about 52 $nCcm^{-2}$) also occurred during the measurement with remnant polarization (P_r of about 30 $nCcm^{-2}$) and a coercive field (E_c) of about 28 $kVcm^{-1}$. The P_s of this compound is very close to that of $KH_2PO_4^-$ type ferroelectrics. The related compound, $[Ni(en)_2(pip)][B_5O_6(OH)_4]_2$, which contains insular oxidoborate anions rather than coordinated oxidoborate ligands, was reported as the first templated oxidoborate with ferroelectric properties [39]. The P_s value for $[Ni(en)_2(pip)][B_5O_6(OH)_4]_2$ of 20 $nCcm^{-2}$ for is signifi-

cantly higher than that of typical organic ferroelectric compounds, e.g., β-quinol-methanol (P_s = 6 nCcm^{-2}). A related pentaborate derivative, $[Zn(dab)_{0.5}(dab')_{0.5}\{B_5O_7(OH)_3\}]_n$ (**40**), has been prepared more recently, and exhibits a wide E_c value of ca. 6 kV cm^{-1} to 11 kV cm^{-1} [8].

Vibrational (IR) data are commonly reported for oxidoborate complexes. In addition to diagnostic bands associated with organic ligands (O-H, N-H, C-C, C-N, C-C etc. stretches and bends) strong absorptions associated with ligand-M and B-O stretches (1400–1000 cm^{-1}) are often observed but usually are not diagnostic since they are in the IR fingerprint region. In general, B-O stretching modes can be subdivided into four specific regions (asymmetric stretches: B_{trig}-O, 1450–1300 cm^{-1}; B_{tet}-O, 1150–1000 cm^{-1}; symmetric stretches: B_{trig}-O, 960–890 cm^{-1}, B_{tet}-O, 890–740 cm^{-1}) with bending and deformation modes at lower energy [40]. Nevertheless, Li and co-workers have tabulated diagnostic wavenumbers for specific smaller oxidoborate anions [40]. Hexaborate(2-) derivatives, with a FBB of 6:(3*D*+3*T*), are fairly common as oxidoborate ligands (e.g., compounds **4**, **5**, **10–12**, **15–20, 42–45**) and diagnostic bands at 955 and 808 cm^{-1} have been proposed for this anion [20,40]. Tentative diagnostic bands (1047, 952, 902 and 857 cm^{-1}) have also been reported for icosaborate(6-) derivatives (**49–51**) [33].

The most studied property of inorganic–organic hybrid borates is their thermal behavior. Indeed, all compounds described within this review, except **10, 12, 33** (which are reported in crystallographic journals [16,18]), have their thermal properties documented. Many of the thermal studies have been undertaken in air from room temperature up to 800 °C, although a few (**4, 23, 24**) report data obtained through heating under N_2 to a similar temperature. Generally, thermal decomposition is a multistage process which includes a low temperature loss of interstitial molecules (where present), a moderate temperature dehydration and cross-linking of oxidoborate hydroxyl groups, and a high temperature oxidation process (or removal of volatile organics) to generate a glassy borate residual solid. This solid can be formulated as an anhydrous metal borate (i.e., a mixed metal/boron oxide) with a M:B ratio that maintains the M:B ratio of the original oxidoborate complex. These principles are illustrated for compounds $[Cd(pn)\{B_6O_7(OH)_6\}]_n{\cdot}nH_2O$ (**4**), $[H_3O]_4[Cu_7(NH_3)_2(H_2O)_4\{B_{24}O_{39}(OH)_{12}\}]{\cdot}13H_2O$ (**13**) and $[Zn(en)\{B_6O_7(OH)_6\}]_n{\cdot}2nH_2O$ (**44**). Compound **44** decomposes thermally (in air) by the loss of 2 interstitial H_2O (100–180 °C), condensation of hydroxyoxidoborate with loss of $3H_2O$ (180–320 °C) and oxidation of the en ligand (320–470 °C) to leave as a residue ZnB_6O_{10} (= $ZnO{\cdot}3B_2O_3$) [34]. Compound **13** thermally decomposes in air by the loss of 21 (interstitial and coordinated) H_2O and 4 (coordinated) NH_3 molecules (at 70–160 °C) and condensation of hydroxyoxidoborate groups with loss of $8H_2O$ (at 160–300 °C) to afford $Cu_7B_{24}O_{43}$ (= $7CuO{\cdot}12B_2O_3$) [19]. Occasionally, the individual processes overlap but the endpoint is the same. Thus, **4** losses weight continuously in one step upon heating, under N_2, from room temperature to 800 °C [11]. In this process the guest water molecules are removed together with pn ligands and the oxidopolyborate fully condenses to afford CdB_6O_{10} (= $CdO{\cdot}3B_2O_3$) [11]. Non-metal cation polyborates have been considered to be thermal precursors to porous materials [5]. To date this has not been successful [41–43] but recent studies on $H_6[Cu_4O\{B_{20}O_{32}(OH)_8\}]{\cdot}25H_2O$ (**20**) and $H_6[Cu_4O\{B_{20}O_{32}(OH)_8\}]{\cdot}34H_2O{\cdot}8B(OH)_3$ (**21**), which contain large 3-D intersecting channel systems with PLATON calculated solvent accessible voids of ca. 60%, suggest that mesoporous materials may be available from hybrid organic oxidoborates [24].

Fire retardancy is often linked to a compound's thermal properties and $[Zn\{B_3O_4(OH)_3\}]_n$ (**35**) [31] is well known for this property and has been commercially exploited. Many zinc borates also possess such properties [44] and the recently prepared hybrid oxidoborate complex $[Zn(H_2O)_6]_2[NO_3]_2{\cdot}[Zn(H_2O)_4\{B_3O_3(OH)_4\}_2]{\cdot}2H_2O$ (**34**) [14] has also been reported as a promising flame retardant, at 15 wt.% loading, for ABS (acrylonitrile butadiene styrene), an important engineering thermoplastic material.

Hybrid metal-organic oxidoborates have been used as precursors to thermally prepared catalysts [9] e.g., carbon material catalysts derived from thermal treatment of

$[Cd(dap)_{0.5}(dap')_{0.5}\{B_5O_8(OH)\}]_n \cdot nH_2O$ (**2**) and $[\{Zn(en)_2\{B_7O_{10}(OH)_3\}_2]_n$ (**46**) have been used to electrochemically reduce CO_2 to CO. Initial results indicate that the oxidoborate is a useful catalyst precursor since at 1.4V CO formation is 51% higher than that of RHE. This may be a promising development as a low-cost alternative to traditional noble metal catalysts.

5. Conclusions

Since metals generally have multiple coordination sites, they often can form coordination linkages with organic (*N*-donor) and oxidoborate (*O*-donor) ligands. These organic/inorganic oxidopolyborate hybrid complexes are structurally diverse and often have polymeric structures based on unique frameworks. The hybrid organic oxidoborate materials in such integrated structures can afford materials with unique properties and which may overcome possible deficiencies inherently present in related single component systems. Hybrid inorganic−organic oxidoborates have attracted considerable recent research attention, and interesting properties such as photoluminescence, ferroelectric and NLO and catalytic properties have been discovered and these are summarized within the review. Initial results indicate that these properties can be tailored and manipulated by adjusting the organic ligands, the oxidoborate motif and/or the central metallic ion, and that such compounds are a promising area for future research.

Author Contributions: Conceptualization, C.-Y.P., M.A.B.; Writing—original draft preparation, C.-Y.P., S.-S.X. and M.-H.Z.; Writing— review and editing, C.-Y.P. and M.A.B.; Funding acquisition, C.-Y.P. All authors have read and agreed to the published version of the manuscript.

Funding: This research was partially funded by the National Natural Science Foundation of China (No. 21671044).

Institutional Review Board Statement: Not applicable.

Informed Consent Statement: Not applicable.

Data Availability Statement: Not applicable.

Conflicts of Interest: The authors declare no conflict of interest. The funders had no role in the design of the study; in the collection, analyses, or interpretation of data; in the writing of the manuscript, or in the decision to publish the results.

Abbreviations

appip	*trans*-1,4-bis(3-aminopropyl)piperazine
dab	1,4-diaminobutane
dap	1,3-diaminopropane
deen	*N*,*N*-diethyl-1,2,-diaminoethane
dmen	*N*,*N*-dimethyl-1,2-diaminoethane
en	1,2-diaminoethane
pip	piperidine
pn	1,2-diaminopropane
py	pyridine
teta	tetraethylenetriamine
tren	tris(2-aminoethyl)amine
tmeda	*N*,*N*,*N*′,*N*′-tetramethyl-1,2-diaminoethane

References

1. Beckett, M.A.; Brellocks, B.; Chizhevsky, I.T.; Damhus, T.; Hellwich, K.-H.; Kennedy, J.D.; Laitinen, R.; Powell, W.H.; Rabinovich, D.; Vinas, C.; et al. Nomenclature for boranes and related species (IUPAC Recommendations 2019). *Pure Appl. Chem.* **2020**, *92*, 355–381. [CrossRef]
2. Christ, C.L.; Clark, J.R. A crystal-chemical classification of borate structures with emphasis on hydrated borates. *Phys. Chem. Miner.* **1977**, *2*, 59–87. [CrossRef]

3. Heller, G. A survey of structural types of borates and polyborates. In *Topics in Current Chemistry*; Springer: Berlin/Heidelberg, Germany, 1986; Volume 131, pp. 39–98. [CrossRef]
4. Grice, J.D.; Burns, P.C.; Hawthorne, F.C. Borate minerals II. A hierarchy of structures based upon the borate fundamental building block. *Canad. Min.* **1999**, *37*, 731–762.
5. Beckett, M.A. Recent Advances in crystalline hydrated borates with non-metal or transition-metal complex cations. *Coord. Chem. Rev.* **2016**, *323*, 2–14. [CrossRef]
6. Schubert, D.M.; Knobler, C.B. Recent studies of polyborate anions. *Phys. Chem. Glasses Eur. J. Glass Sci. Technol. Part B* **2009**, *50*, 73–78.
7. Jin, S.S.; Cai, G.; Wang, W.; He, M.; Wang, S.; Chen, X. Stable oxoborate with edge-sharing BO_4 tetrahedra synthesized under ambient pressure. *Angew. Chem. Int. Ed. Engl.* **2010**, *122*, 5087–5090. [CrossRef]
8. Zhi, S.-C.; Wang, Y.-L.; Sun, L.; Cheng, J.-W.; Yang, G.-Y. Linking 1D transition-metal coordination polymers and different inorganic boron oxides to construct a series of 3D inorganic−organic hybrid borates. *Inorg. Chem.* **2018**, *57*, 1350–1355. [CrossRef]
9. Liu, Y.; Zhou, K.; Chen, H.-L.; Gong, Y.-N.; Pan, C.-Y. A Way for Derived Carbon Materials by Thermal Etching Hybrid Borate for Electrochemical CO_2 Reduction. *Inorg. Chem.* **2020**, *59*, 10785–10793. [CrossRef]
10. Pan, R.; Chen, C.-A.; Bai-Feng Yang, B.-F.; Yang, G.-Y. Two New Octaborates Constructed of Two Different Sub-clusters and Supported by Metal Complexes. *J. Clust. Sci.* **2017**, *28*, 1237–1248. [CrossRef]
11. Deng, J.-X.; Zhou, K.; Pan, C.-Y. The tunable luminescent property and wide band gap in three 1D hybrid templated borates containing different metallic ions and oxoboron clusters. *J. Solid State Chem.* **2020**, *281*, 121042. [CrossRef]
12. He, Y.; Liu, Y.; Xin, S.-S.; Pan, C.-Y. Trinuclear Cd_3O_{14} hexaborate and two nickel borates based on molten salt synthesis and precursor synthesis: Structure, characterization, and properties. *Dalton Trans.* **2020**, *49*, 14640–14646. [CrossRef]
13. Wei, Q.; Zhang, Y.-J.; Song, Y.; Yang, G.-Y.; Zou, X. A series of inorganic–organic hybrid cadmium borates with novel Cd-centred $[Cd@B_{14}O_{20}(OH)_6]^{2-}$ clusters. *Dalton Trans.* **2016**, *45*, 13937–13943. [CrossRef]
14. Liu, Y.; Deng, J.-X.; Pan, C.-Y. Synthesis and structural manipulation of a polyanionic zincoborate $[Zn(H_2O)_6](NO_3)_2[Zn\{B_3O_3(OH)_4\}_2(H_2O)_4]\cdot 2H_2O$ by the molten salt method and its potential application as a flame retardant. *J. Clust. Sci.* **2020**, *281*, 121042. [CrossRef]
15. Wang, G.-M.; Sun, Y.-Q.; Yang, G.-Y. Syntheses and crystal structures of three new borates templated by transition-metal complexes in situ. *J. Solid State Chem.* **2006**, *179*, 1545–1553. [CrossRef]
16. Jemai, N.; Rzaigui, M.; Akriche, S. Piperazine-1,4-diium bis-(hexahydroxidoheptaoxidohexaborato-κ^3O,O′,O′′)cobaltate(II) hexahydrate. *Acta Cryst.* **2014**, *70*, m167. [CrossRef] [PubMed]
17. Jemai, N.; Rzaigui, M.; Akriche, S. Stabilization of hexaborate net with mixed Co(II) metal and organic cations: Synthesis, rationale characterization, comparative study and enhancement of the bioactivity. *J. Clust. Sci.* **2015**, *26*, 2051–2064. [CrossRef]
18. Lan, S.M.; Di, W.-J.; Shao, Z.-D.; Liang, Y.-X. Two new transition metal inorganic–organic hybrid borates: [*tris*-(2-aminoethoxy)trihydroxyhexaborato]cobalt(II) and its nickel(II) analogue. *Acta Cryst.* **2011**, *C67*, m338–m341. [CrossRef]
19. Altahan, M.A.; Beckett, M.A.; Coles, S.J.; Norton, P.N. Synthesis and characterization by a single-crystal XRD study of $[H_3O]_4[Cu_7(NH_3)_2(H_2O)_4\{B_{24}O_{39}(OH)_{12}\}]\cdot 13H_2O$: An unusual bis(hydroxytrioxidoborate) tri-metallic chain supported by a $[\{Cu_4O\}\{B_{20}O_{32}(OH)_8]^{6-}$ cluster. *J. Clust. Sci.* **2018**, *29*, 1337–1343. [CrossRef]
20. Altahan, M.A.; Beckett, M.A.; Coles, S.J.; Norton, P.N. Synthesis and characterization of polyborates templated by cationic copper(II) complexes: Structural (XRD), spectroscopic, thermal (TGA/DSC) and magnetic properties. *Polyhedron* **2017**, *135*, 247–257. [CrossRef]
21. Hathaway, B.J.; Hodgson, P.G. Copper-ligand bond-lengths in axial complexes of copper(II) ion. *J. Inorg. Nucl. Chem.* **1973**, *35*, 4071–4081. [CrossRef]
22. Altahan, M.A.; Beckett, M.A.; Coles, S.J.; Norton, P.N. Copper(II) complexes of hydroxyoxidoborates. Synthesis and characterization of two clusters containing the hexaborate(2-) ligand: $[Cu(NH_2CH_2CH_2NEt_2)\{B_6O_7(OH)_6\}]\cdot 5H_2O$ and $[Cu(NH_3)_2\{B_6O_7(OH)_6\}]\cdot 2H_2O$. *J. Clust. Sci.* **2019**, *30*, 599–605. [CrossRef]
23. Altahan, M.A.; Beckett, M.A.; Coles, S.J.; Norton, P.N. Oxidopolyborate chemistry: The self-assembled, templated, synthesis and an XRD study of a 1-D coordination polymer $[Cu(en)\{B_6O_7(OH)_6\}]\cdot 3H_2O$. *Phosphorus Sulfur Silicon Rel. Elem.* **2020**, *195*, 952–956. [CrossRef]
24. Wang, J.-J.; Wei, Q.; Yang, B.-F.; Yang, G.-Y. Two new copper borates with mesoscale cubic supramolecular cages assembled from $\{Cu_4@B_{20}\}$ clusters. *Chem. Eur. J.* **2017**, *23*, 2774–2777. [CrossRef] [PubMed]
25. Hu, T.; Hu, C.-L.; Kong, F.; Mao, J.-G.; Mak, T.C.W. Exploratory investigation of new SHG materials based on galloborates. *Inorg. Chem.* **2012**, *51*, 8810–8817. [CrossRef]
26. Cheng, L.; Yang, G.-Y. A series of novel gallium and indium borates constructed from $[B_5O_8(OH)_2]^{3-}$ clusters and metal complex linkers. *J. Solid. State Chem.* **2013**, *198*, 87–92. [CrossRef]
27. Zhang, H.-X.; Zhang, J.; Zheng, S.-T.; Yang, G.-Y. $K_7\{(BO_3)Mn[B_{12}O_{18}(OH)_6]\}\cdot H_2O$: First manganese borate based on covalently linked $B_{12}O_{18}(OH)_6$ clusters and BO_3 units $_{via}$ Mn^{2+} cations. *Inorg. Chem. Commun.* **2004**, *7*, 781–783. [CrossRef]
28. Altahan, M.A.; Beckett, M.A.; Coles, S.J.; Norton, P.N. Oxidoborates templated by cationic nickel(II) complexes and self-assembled from $B(OH)_3$. *Inorganics*. Manuscript in preparation.
29. Schubert, D.M.; Alam, F.; Visi, M.Z.; Knobler, C.B. Structural characterization and chemistry of the industrially important zinc borate, $Zn[B_3O_4(OH)_3]$. *Chem. Mater.* **2003**, *15*, 866–871. [CrossRef]

30. Paul, A.K.; Sachidananda, K.; Naterajan, S. $[B_4O_9H_2]$ Cyclic borate units as the building unit in a family of zinc borate Structures. *Cryst. Growth Des.* **2010**, *10*, 456–464. [CrossRef]
31. Zhao, P.; Cheng, L.; Yang, G.-Y. Synthesis and characterization of a new organic-inorganic hybrid borate: $[Zn(dab)_{0.5}(dab')_{0.5}(B_4O_6(OH)_2)]\cdot H_2O$. *Inorg. Chem. Commun.* **2012**, *20*, 138–141. [CrossRef]
32. Wang, G.M.; Sun, Y.-Q.; Yang, G.-Y. Synthesis and crystal structures of two new pentaborates. *J. Solid State Chem.* **2005**, *178*, 729–735. [CrossRef]
33. Altahan, M.A.; Beckett, M.A.; Coles, C.J.; Horton, P.N. Hexaborate(2-) and dodecaborate(12-) anions as ligands to zinc(II) centres: Self-assembly and single crystal XRD characterization of $[Zn\{k^3\text{-}O\text{-}B_6O_7(OH)_6\}(\kappa^3\text{-}N\text{-dien})]\cdot 0.5H_2O$ (dien = $NH(CH_2CH_2NH_2)_2$), $(NH_4)_2[Zn\{\kappa^2\text{-}O\text{-}B_6O_7(OH)_6\}(H_2O)_2]\cdot 2H_2O$ and $(1,3\text{-pn})_3[(\{\kappa^1\text{-}NH_3\{CH_2\}_3NH_2)Zn\{\kappa^3\text{-}O\text{-}B_{12}O_{18}(OH)_6\}]_2\cdot 14H_2O$. *Inorganics* **2019**, *7*, 44. [CrossRef]
34. Altahan, M.A.; Beckett, M.A.; Coles, C.J.; Horton, P.N. Two 1-D Coordination Polymers containing Zinc(II) Hexaborates: $[Zn(en)\{B_6O_7(OH)_6\}]\cdot 2H_2O$ (en = 1,2-diaminoethane) and $[Zn(pn)\{B_6O_7(OH)_6\}]\cdot 1.5H_2O$ (pn = (+/−)-1,2-diaminopropane). *Crystals* **2018**, *8*, 470. [CrossRef]
35. Rong, C.; Jiang, J.; Li, Q.-L. Synthesis of transitional metal borate $K_7\{(BO_3)Zn[B_{12}O_{18}(OH)_6]\}\cdot H_2O$ and Quantum Chemistry Study. *Chin. J. Inorg. Chem.* **2012**, *28*, 2217–2222.
36. Altahan, M.A.; Beckett, M.A.; Coles, C.J.; Horton, P.N. Transition-metal complexes with oxidoborates. Synthesis and XRD characterization of $[(H_3NCH_2CH_2NH_2)Zn\{\kappa^3O,O',O''\text{-}B_{12}O_{18}(OH)_6\text{-}\kappa^1O''\}$ $Zn(en)(NH_2CH_2CH_2NH_3)]\cdot 8H_2O$: A neutral bimetallic zwiterionic polyborate system containing the 'isolated 'dodecaborate(6-) anion. *Pure Appl. Chem.* **2018**, *90*, 625–632. [CrossRef]
37. Corbett, P.T.; Leclaire, J.; Vial, L.; West, K.R.; Wietor, J.-L.; Sanders, J.K.M.; Otto, S. Dynamic combinatorial chemistry. *Chem. Rev.* **2006**, *106*, 3652–3711. [CrossRef]
38. Pan, C.Y.; Zhong, L.J.; Zhao, F.H.; Luo, Y.Z.; Li, D.G. Cotemplating synthesis of a rare borate $Ni(en)_3\cdot Hen\cdot[B_9O_{13}(OH)_4]\cdot H_2O$ with a chiral polyanonic chain Constructed from two different clusters. *Inorg. Chem.* **2015**, *54*, 403–405. [CrossRef] [PubMed]
39. Pan, C.Y.; Hu, S.; Li, D.G.; Ouyang, P.; Zhao, F.H.; Zheng, Y.Y. The first ferroelectric templated borate: $[Ni(en)_2pip][B_5O_6(OH)_4]_2$. *Dalton Trans.* **2010**, *39*, 5772–5773. [CrossRef] [PubMed]
40. Li, J.; Xia, S.; Gao, S. FT-IR and Raman spectroscopic study of hydrated borates. *Spectrochem. Acta* **1995**, *51A*, 519–532. [CrossRef]
41. Beckett, M.A.; Horton, P.N.; Hursthouse, M.B.; Timmis, J.L.; Varma, K.S. Templated heptaborate and pentaborate salts of cyclo-alkylammonium cations: Structural and thermal properties. *Dalton Trans.* **2012**, *41*, 4396–4403. [CrossRef]
42. Beckett, M.A.; Horton, P.N.; Hursthouse, M.B.; Knox, D.A.; Timmis, J.L. Structural (XRD) and thermal (DSC, TGA) and BET analysis of materials derived from non-metal cation pentaborate salts. *Dalton Trans.* **2010**, *39*, 3944–3951. [CrossRef] [PubMed]
43. Beckett, M.A.; Horton, P.N.; Hursthouse, M.B.; Knox, D.A.; Timmis, J.L. Triborate and pentaborate salts of non-metal cations derived from *N*-substituted piperazines; Synthesis, structural (XRD) and thermal properties. *RSC Adv.* **2013**, *3*, 15185–15191. [CrossRef]
44. Schubert, D.M. Hydrated zinc borates and their industrial use. *Molecules* **2019**, *24*, 2419. [CrossRef] [PubMed]